

Evaluation of Intelligent Solar Based Hand Gesture Controlled Lawn Robot

Adefemi O. Adeodu ^{1*}, Rendani W. Maladzi ¹, and Mukondeleli G. Kana-kana Katumba ²

¹ Department of Mechanical Engineering, University of South Africa, Florida, South Africa;
Email: maladrw@unisa.ac.za (R.W.M.)

² Department of Industrial Engineering, Tshwane University of Technology, Pretoria, South Africa;
Email: KanakanaMG@tut.ac.za (M.G.K.K.)

*Correspondence: eadeodao@unisa.ac.za (A.O.A.)

Abstract—Hand gesture interpretation and control in robotics describe the interconnection between human and machine elements in the computer vision world. The pruning of a structured environment is time-consuming and labour-intensive. Therefore, it requires to be managed by a self-propelled machine. A path planning mode allows the robot to move along a specified path and various studies on lawn robots focus more on obstacle avoidance with limited consideration to proper path planning techniques. Hand gesture interpretation and control is implemented to solve the challenge of path definition. This study is targeted at the development of a solar powered lawn robot using hand gesture control as path planning technique. The robotic system continuously operates using charged batteries via solar energy stored in photovoltaic cells. The robot control mechanism was implemented via the use of infrared sensors to avoid obstruction on its path and hand gesture interpretation via digital signal processing (DSP) for the path planning. The performance evaluation of the robot was based on field experiment and simulation using solid works, defined in terms of area of covered lawn availability, energy utility and optimum turning velocity. The evaluation revealed that the machine's efficiency is almost 100% based on area covered, percentage availability of the robot is 95% and an average energy utility of 7.7 KWh was also obtained. The optimum turning velocity of 0.096 m/s at work completed time of 20 minutes were obtained by simulation. This robot is found useful for any environment, both structured and semi-structured.

Keywords—area covered, digital signal processing, hand gesture, robotic, obstacle avoidance

I. INTRODUCTION

Hand gesture recognition and interpretation in robotics is a class of machine-human interaction implemented in the field of computer when dealing with path planning. On this basis, robotic systems take definite instructions for carrying out task relative to directions. A gesture identification and interpretation study distinguishes a defined body movement and communicates the message to the user in

order to establish the link between human and machine [2, 3].

Hand gesture control finds a wide range of applications in telerobotic, where machine systems are naturally manipulated with such telerobotic communication [4–6] to serve information relating to directions to the machine such as left, right, etc. Application in the lawn cutting robot is a simple and unique method of controlling the geometric movement of the robot as a means of path planning. The aesthetic value maintenance of an environment, structured or semi-structured, is generally labour-intensive and time-consuming [1], therefore the need for executing the task effectively is of utmost important.

Researches are being done in this area where several approaches have been developed for hand movement sensing and robotic control [7–9]. A haptic glove with teleoperation study was carried out by Ma [10], which captures the movements of each finger in operations. A virtual robot teleoperation dependent of hand gesture identification was demonstrated by Li [11]. The classification was done via adaptive Neuro-Fuzzy inference systems and support vector machine (SVM). A robotic surgery dependent on augmented reality was executed by Wen [12], in which the implementation of specific radio frequency needles in successive plans was carried out using hand gesture.

Greenfield [13] discusses touchless device, controlled and implemented by hand gesture based on recognition of the optical pattern of hand motions. DU [14] demonstrated the robotic manipulator via hand gesture. Kalman and particle filters were used. Although it was a markerless method it used leap motion to detect hand positions. Also, a hand gesture controlled TV was built by Samsung [15].

The contribution of the work was demonstrated by hand gesture configuration for defining the path of the solar grass cutting robot, adapted for both handicap and non-handicap users by show of hand movement in front of a high resolution camera linked to a digital signal processing (DSP)-based embedded board, whereby the image is being

Manuscript received June 21, 2022; revised July 27, 2022; accepted November 11, 2022.

This work is an extension of work originally presented in ICAST Adeodu *et al.* [1]

n captured in real time. An algorithm based on a DSP processor TMS320DM642EVM implementation was used to evaluate actuation via many hand gestures without contact to the surface of the screen. Real-time performance is made possible which extended the limit of applications to include ones with a high frame rate.

II. SYSTEM ARCHITECTURE AND DESCRIPTION

The robot uses were captured in frames using a stream of live videos in fixed time range for gesture control. This is based on a natural computing concept made available to anyone irrespective of hand anthropometry [2, 3]. Gestures were classified based on the principle of analysis of components, implemented in embedded Matlab, Simulink and Code Composer Studio (CCS). An XDS 560 PCI JTAG Emulator was fitted in a PCI slot to enhance high speed RTDX on the enabled processor for transfer of data over a tune of 2 Mb per second [2, 3]. Other features are as applicable to the robot developed in Adeodu *et al* [1]. Figs. 1 and 2 show the flow process diagram of the robot hand gesture control and the block diagram respectively. Table I presents the components and specifications for the robot

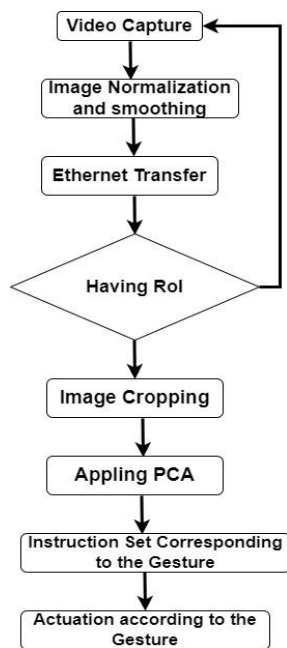


Figure 1. Process flow diagram for robot hand gesture control [2]

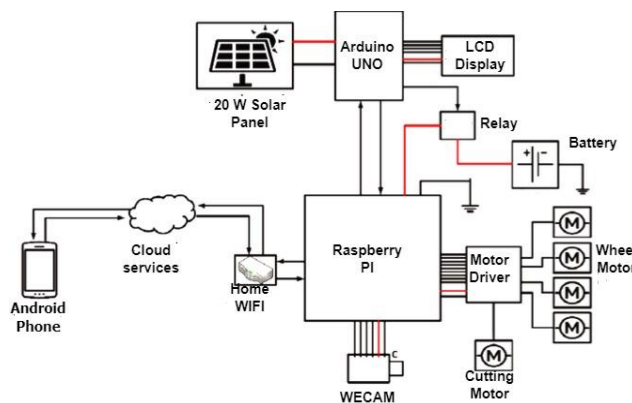


Figure 2. Block Diagram of the robot [1]

TABLE I. ROBOT COMPONENT AND SPECIFICATION

S/N	Component	Specification
1	Solar Panel	18v (20watts)
2	DC Motor for cutter	3000 rpm (12V, 700 mA)
3	Batteries	Lithium cell 12v (10Ah)
4	LCD Screen	16 by 2 and 5 by 7 pixel matrix
5	Microcontroller	ATmega 328 arduino Output PCB A-13400-3
6	High Resolution Camera	Model RF625 Range from 5 to 1400mm Linearity in the range of ± 0.1
7	Infrared Sensor	Model HC-SR04 Range of 2 to 400cm Accuracy over 3mm
8	Blade	Stainless steel Thickness is 0.5mm
9	Wheel of the Robot, DC Motors and Gears	BLDC 300rpm
10	DSP Processor	TMS320DM642EVM

III. SYSTEM DESIGN

Obstacle avoidance and hand gesture control modules are the main design architecture for the robot. The robot navigates along a defined path avoiding collision against any obstruction

A. Design of Module for the Obstacle Avoidance

This is arranged such that colour and distance are detected via infrared sensors TCRT5000 using echo resounding technique. The IR sensors emit waves which detect obstacles at a range when the echo of the reflected wave is received. The detailed module design and connection were presented in Adeodu *et al* [1]. The flow chart of the module is shown in Fig. 3. Also, Figs. 4 and 5 present the adopted programming and circuit diagram respectively.

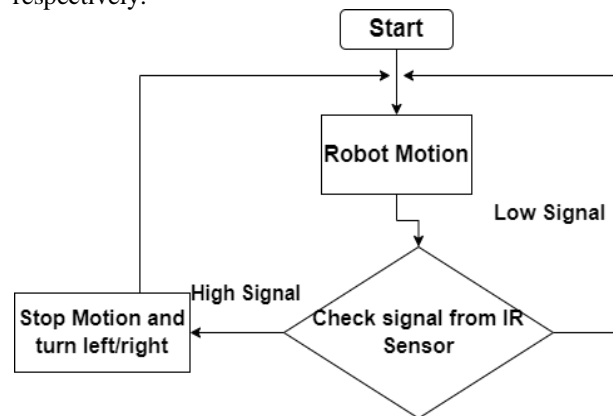


Figure 3. Flow diagram module for obstacle avoidance [1]

```

sketch_jul13a$
long cm, duration;
const int echoPin = 11;
const int trigPin = 12;
const int lm1 = 5;
const int lm2 = 6;
const int lspeed = 9;
const int rml = 7;
const int rm2 = 8;
const int rspeed = 10;
int spd=255;
// Above sets the speed of the bot
void setup()
{
  pinMode(lm1, OUTPUT);
  pinMode(lm2, OUTPUT);
  pinMode(rm1, OUTPUT);
  pinMode(rm2, OUTPUT);
  pinMode(lspeed, OUTPUT);
  pinMode(rspeed, OUTPUT);
  pinMode(trigPin, OUTPUT);
  pinMode(echoPin, INPUT);
  analogWrite(lspeed, spd);
  analogWrite(rspeed, spd);
  Serial.begin(9600);
}
void loop()
{

```

Figure 4. Programming coding for obstacle avoidance [1]

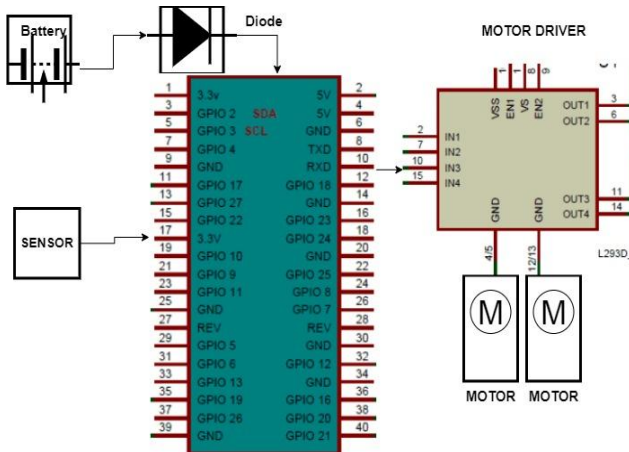


Figure 5. Circuit diagram of module for obstacle avoidance [1]

B. Module for Hand Gesture Control

The design for hand gesture control of the robot was implemented in four stages via an embedded Matlab, Simulink and code composer studio [2].

C. Gesture Extraction from Video Stream

Image capture and pre-processing were carried out frame by frame per one-fifth second. The image smoothing and normalisation were executed within the DSP board as shown in Fig. 6. Additional information on smoothing and normalisation are discussed in [16, 17]. A large reduction for the algorithm was done by the board in the execution time, after which the image frame was sent to PC via user datagram protocol (UDP) target to HOST Ethernet communication in Fig. 7. Fig. 8 shows the transfer of the data from PC to host [2].

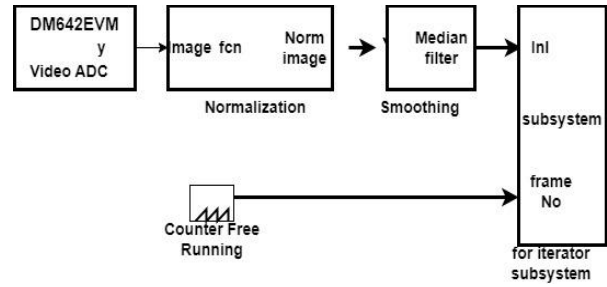


Figure 6. Smoothing and Normalization of DSP [3]

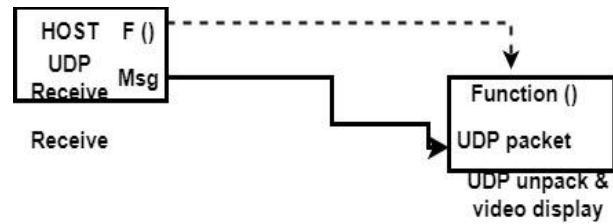


Figure 7. UDP Target to the Host [3]

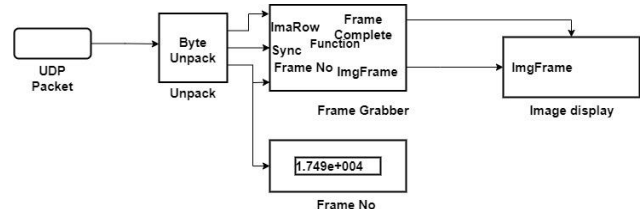


Figure 8. Data Transfer to the Host [3]

D. Extraction of Region of Interest from the Frame

This aspect is normally referred to as Cropping, where the unwanted information from the selected frame is removed. The selected frame was changed to a binary image using global thresholding [2]. Fig. 9 shows the hand gesture frame prior to and after cropping.

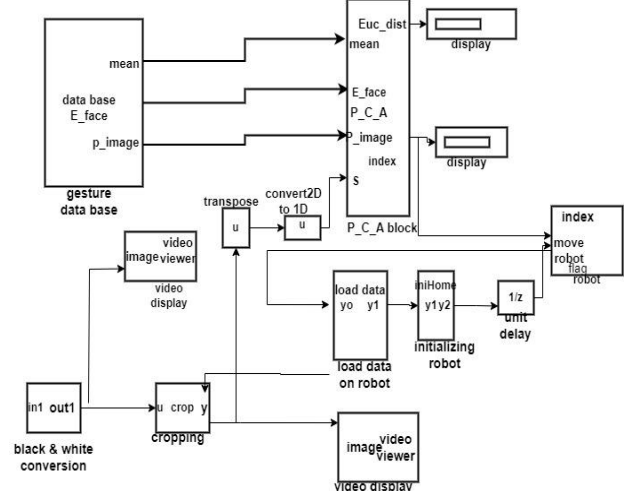


Figure 9. Image after Pre-processing [3]

E. Determination of Gesture and Pattern Matching

The principle of component analysis (PCA) is more desirable for pattern matching compared to other methods such as Artificial Neural Network (ANN), which needs

longer processing time [18]. It is to be noted that cropped images were resized to match data-based images.

F. Generation of Control Instruction for the Robot

The pattern for a particular gesture is written and stored in the data base. Different hand gestures of up to six were used for the design of a particular move of the robot in precise angle and direction [3]. A gesture is presented in front of the robot, captured by the camera. This is processed and matched with those in the data base. The action that corresponded to the gesture was processed and sent to the robot for action.

G. Image Processing and Improvement

This aspect is not a major sub-module of hand gesture control module. It comes in between the extraction of region of interest and determination of gesture pattern. This is the point where the image quality is improved with reference to pixel value. It is carried out by the interaction between AT Mega Arduino Uno microcontrollers and a Matlab graphical user interface (GUI) based image editor. The microcontroller comes with pre-programmed and a boot loader that allows the user to unload the new code [19]. Image processing is divided into image compression, image enhancement and restoration, and measurement extraction [19]. A defect in image quality is caused either by digitisation or by faults in the set-up. This is corrected by image enhancement, once good condition, measurement extraction is used to obtain good information such as colour and tracking. Matlab GUI for image enhancement is made with a computer which runs the matlab program and Arduino Uno microcontroller board. This controls the robot by controlling the action of the motor driver circuit as the user controls the motor through hand gesture. Communication between the computer and Arduino is via wireless system.

H. Image Colour Tracking Process

The image movement frame with respect to colour is taken as input. This processing is the fundamental part of tracking that uses matlab coding [19]. Matlab tracks the colour of the image movement direction (command) and sends it directly to the Arduino Uno microcontroller via communication with the Arduino software. Assisted by the motor driver circuit, the Arduino controls the movement of the robot in the required direction as given by the command. The image colour is interpreted as RGB format [2] [19] by the matlab programme that is to be processed. The RBG images are flipped in both rows and columns to correct the effect of flipped images taken by the camera. Then, the particular colour upon which the matlab colour tracking programme is based is extracted. The image also contains dusty noise, which is filtered by median filter [19]. This monochromatic image is then converted to black and white [19]. From the image, area, centroid coordinates and bounding box containing the colour used for a particular command are easily determined. The changes in x and y coordinates represent the movement of hand along x and y axis, i.e, right or left and upward or downward, respectively. The tracking programme functions thus; the programme tracks the centroid and bounding box, based on the

direction of movement of the centroid. The programme communicates the direction command via software to the robot. Consideration is given that hand gesture movement is never absolutely in a particular direction, but a random threshold of other coordinates is taken to omit the changes before the command is passed to the robot [19].

I. Load Design Consideration

The load design consideration for the solar-powered lawn robot took into consideration the design of the solar panel, design of the cutting unit and chassis design.

1) Design of the chassis

The material selected for the construction of the chassis of the grass cutting robot is plastic as it will be exposed to intermittent sunlight and water. The material was selected based on its desirable properties such as resistance to corrosion, high strength-to-weight ratio, durability, low cost and low toxicity. Aluminium beams were used to create support for the robot chassis. The lawn robot has a standard weight of 400 N (40kg), which comprises the chassis frame, batteries, solar panel and other mountings. This will determine the amount of torque required for easy movement of the robot wheel.

2) Power requirement for lawn robot movement

The tractive force required for the motion of the lawn robot depends on the following three factors [20]:

Rolling Resistance (Rr) is the force required to keep the wheel rolling [21] and is expressed as Eq. (1)

$$R_r = W \times C_r = 400 \times 0.075 = 30 \text{ N} \quad (1)$$

where Rr = Rolling Resistance (N)

W = Weight of the Robot (N)

Cr = Coefficient of Rolling Resistance (grass surface = 0.075) [21]

Gradient Resistance (Rg) is the force due to gravity which causes resistance to the motion of the robot up a slope [21] and it's expressed as Eq. (2).

$$R_g = W \sin \theta = 400 \sin 0.0175 = 7 \text{ N} \quad (2)$$

The slope angle (θ) is taken as 1°

Acceleration Force (Fa) is the force that supports the robot to attain a particular speed. Safe mowing speed of a lawn robot is taken as 5.31Km/hr (1.475 m/s) at a constant velocity to be achieved in the first 5 seconds of starting the lawn robot [21]. The acceleration of the robot is thus calculated as 0.295 m/s^2 .

$$F_a = Ma = 40 \times 0.295 = 11.8 \text{ N} \quad (3)$$

where M is the mass of the robot

The total tractive force is the force needed to freely move the robot and is expressed as:

$$F_t = R_r + R_g + F_a = 30 + 7 + 11.8 = 48.8 \text{ N} \quad (4)$$

The torque to actuate the movement of the wheel is expressed as Eq. (5).

$$\tau = F_t \times r_w = 48.8 \times 0.1016 = 4.96 \text{ N} \quad (5)$$

where r_w is the radius of the wheel

Power requirement for the movement of the lawn robot is expressed in Eq. (6) as:

$$P = \tau \left(\frac{2\pi N}{60} \right) = 4.96 \left(\frac{2 \times 3.142 \times 3000}{60} \right) 1558.4 \text{ watt} \quad (6)$$

3) Design of the cutting unit

The working principle governing the operation of the machine is due to impact and shearing action. For smooth grass cutting, a motor power of not less than 0.83 Hp with rotating speed not less than 3000 rpm producing shear force of about 10.5 N is recommended [22]. The blade is flat shaped with sharp cutting edge for easy cutting. It's fixed perpendicularly beneath the DC motor, rotating at 360° [23].

The peripheral speed of the blade is expressed as Eq. (7):

$$V = \left(\frac{\pi d N}{60} \right) = \left(\frac{3.142 \times 0.3048 \times 3000}{60} \right) 47.88 \text{ m/s} \quad (7)$$

where V is the Blade Speed (m/s)

d is the Diameter of the Blade (mm)

N is the Shaft Speed (rpm)

Consideration for cutting blade selection and computation of torque for the rotation of the blade is presented below. Considering the movement through a square meter unit area of the lawn, the blade dimensions of 0.005 m × 0.009 m × 0.005 m (length, width and thickness) was selected. Volume (V) of the blade is obtained as expressed in Eq. (8).

$$V_b = 0.005 \times 0.009 \times 0.005 = 2.25 \times 10^{-7} \text{ m}^3 \quad (8)$$

The blade is made of stainless steel of density (ρ) of 8000 kg/m³. Thus, weight of the blade is calculated as

$$W_b = \rho g V_b = 8000 \times 10 \times 2.25 \times 10^{-7} = 0.018 \text{ N} \quad (9)$$

The minimum torque to rotate the blade is expressed as Eq. (10).

$$\tau_b = W_b \times X_{rb} = 0.018 \times 0.015 = 2.7 \times 10^{-4} \text{ N/m} \quad (10)$$

Power generated by the blade is expressed as Eq. (11).

$$P_b = \tau_b \left(\frac{2\pi N}{60} \right) = 2.7 \times 10^{-4} \times 314.2 = 0.084 \text{ watt} \quad (11)$$

Shear Force (F) is expressed as Eq. (12).

$$F = \frac{\tau_b}{r_b} = \frac{2.7 \times 10^{-4}}{0.015} = 0.018 \text{ N} \quad (12)$$

where F = Shear Force (N)

τ_b is the Shaft Torque (Nm)

r_b is the Radius of the Blade (mm)

P is the Power developed by shaft (Watt)

4) Solar power sizing

In selecting the solar panel, the following were considered;

- i. The average sun hours per day (isolation).
- ii. Size of the battery.
- iii. Current draw of the motor.

Frequency and duration of use of the mower.

The solar panel is 0.35 m × 0.25 m with specifications of 18 V, 20 W. The batteries selected were two 10 Amp, 12 Volt rechargeable lead acid batteries. To charge this fully, a 20 Watt, 18 volts solar panel would suffice. This panel has a resistance of 3 ohms, which gives an amperage of 18/3 = 6 amps, which is less than the selected battery

amperage of 10 Amps. The solar panel only powers the batteries; that is, the blade and wheels.

IV. EVALUATION OF THE ROBOT

The efficiency of the machine was examined based on parameters such as area covered, availability on the lawn and energy consumption, on a standard lawn with a maximum slope angle of approximately 2° for five hours in the day time. Major necessary measures for maximum performance and smooth operation relating to installations according to design were fully implemented before the start of the test. The cutting range of the machine was adjusted to the standard height of 45mm. It's assumed that in a situation of less interruption with little effect on the machine operation, time is disregarded, else the time which the robot stops is added to the total time. The machine is permitted to touch the soft obstacles but not the rigid obstacles [22]. Fig. 10 shows the Lawn area covered by the robot.

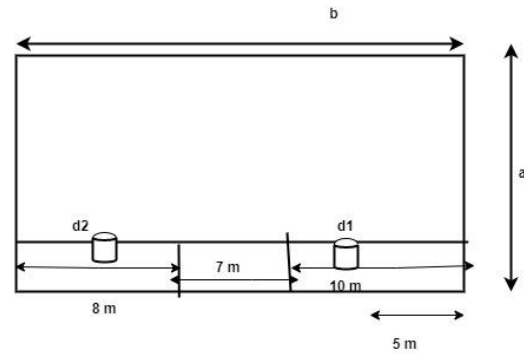


Figure 10. Lawn area.

Lawn Size (A_l) is 196 m², lawn breadth (a) is 8 m and length (b) is 25 m; x is rigid wall of 3m height

d_1 = soft obstacle of 1 m diameter,

d_2 = rigid obstacle of 1 m diameter with 140 mm minimum height

A. Area Coverage Evaluation

At the end of the cutting exercise, all uncut areas fully within 100 mm diameter circle were disregarded, while all uncut areas not in the 100 mm circle and the area uncut in front of rigid obstacles were significant and estimated to be assumed as a rectangle having the dimensions of aui and bui. The section of the covered and uncovered areas is shown in Fig. 11. Table II shows the estimation of the uncut area.

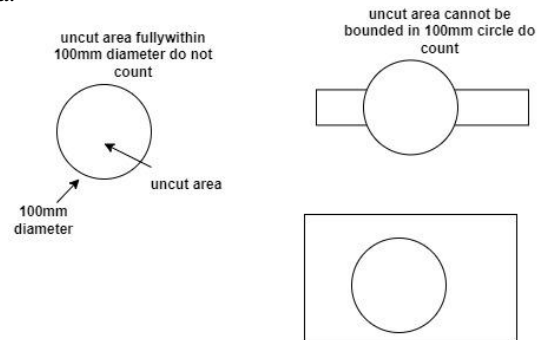


Figure 11. Diagram of covered and uncovered areas [1]

$$A_{ut} = \sum_{i=1}^n (a_{ui} \times b_{ui}) = (a_{u1} \times b_{u1}) + (a_{u2} \times b_{u2}) + \dots (a_{un} \times b_{un}) \quad (13)$$

$$C_A = \frac{A - A_{ut}}{A_t} \times 100 \quad (14)$$

where C_A is the Covered Area
 A_t is the Total Lawn Area
 A_{ut} is the Total Uncut Area
 a_{ui} and b_{ui} are the dimensions of the uncut areas in different locations

TABLE II. EVALUATION OF UNCUT AREA [1]

Uncut location	a_u (m)	b_u (m)	A_{ut} (m ²)
Location 1	0.20	0.15	0.030
Location 2	0.15	0.30	0.044
Location 3	0.35	0.20	0.070
		Total	0.144

$$C_A = \frac{196 - 0.144}{196} \times 100 = 99.9 \% \quad (15)$$

The result from Table II indicates that total area uncut is 0.144 m², and percentage covered area of 99 % is achieved. This shows good performance of the robot after final duration.

B. Estimation of Lawn Availability and Machine Intervention

There was a total time off of 15 minutes for a periodic check on the machine.

$$T_{off} = \sum_{i=1}^n T_{off}(i) = T_{off}(1) + T_{off}(2) \dots + T_{off}(n) \quad (16)$$

$$T_A = \frac{\sum T_{off}(i)}{5hrs} \times 100 \quad (17)$$

where T_{off} is the Total Time off
 T_A is the Lawn Availability

$$T_{off} \times 5 \times 3 = 15 \text{ Minutes} \quad (18)$$

$$\% T_{off} = \frac{15}{5 \times 60} \times 100 = 5 \% \quad (19)$$

$$\% T_A = 100 - 5 = 95 \% \quad (20)$$

The result indicates that percentage lawn availability based on total time off of the machine is 95 %. Low percentage of total time off of the machine was due to the design of the machine as solar-powered. Hence, less interruption in the operation time.

C. Estimation of Energy Consumption of the Robot

Energy consumption (E_c) in Wh is expressed as:

$$E_c = P \times T = 1558.4 \times 5 = 7792 \text{ Wh} \quad (21)$$

where P = Power Requirement by the robot
 t = Total time of operation

There is good energy input for the machine consumption due to majority of solar energy stored the battery being

converted to mechanical energy for rotating the cutting blade and movement of the robot wheel.

D. Performance Simulation

Simulation of the performance evaluation of the solar powered hand gesture controlled lawn robot was carried out using Solid Works 2021 premium software. This is used to examine the variations of work completion time and centrifugal force experienced by the robot against turning velocity to determine the optimum turning velocity by the robot that will maximise cutting without losing its stability and deviating from the specified path. Fig. 12, presents the lawn model and its operational details.

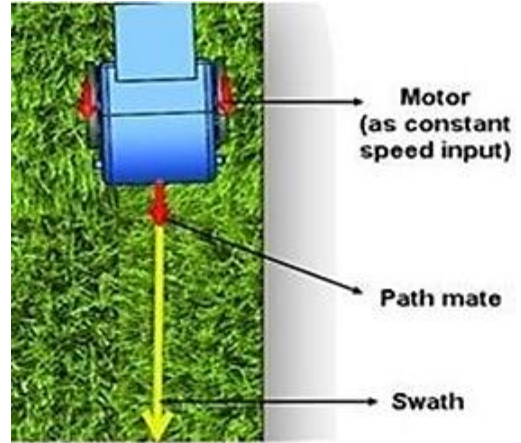


Figure 12. Lawn model and operational details

The work completion time was obtained by calculating the ratio of total distance covered by the robot (area coverage) to the mowing speed. The total distance covered is calculated as the perimeter of the rectangular path traced [21]. According to the blade design of the lawn robot, the length of the blade is 0.005m. Hence, a cut ratio of 1 to 0.55 per square meters is assumed to be achieved. Therefore, total area covered for the entire lawn of 196 sq. m is thus calculated. Table III presents the results of the simulation

$$C_A = 196 \times 0.55 = 107.8 \quad (22)$$

The expression for work completion time is given as Eq. (23).

$$t_{wc} = \frac{107.8}{v \times 60} \quad (23)$$

Also, the expression for centrifugal force is given as Eq. (24).

$$F_c = \frac{mv^2}{r} \quad (24)$$

where C_A = Covered Area (m)
 t_{wc} = Work completion time (s)
 v = Mowing Velocity (m/s)
 m = Mass of the Robot (kg)
 F_c = Centrifugal force (N)
 r = Radius of Curvature is taken as 0.2 m

TABLE III. RESULTS OF THE PERFORMANCE SIMULATION

S/N	Mowing Velocity (v) (m/s)	Work Completion Time (t_{wc}) (Min)	Centrifugal Force (F_c) (N)
1	0.0199	90.284757	0.079202
2	0.0398	45.142379	0.316808
3	0.0598	30.044593	0.715208
4	0.0797	22.542869	1.270418
5	0.0997	18.020729	1.988018
6	0.1196	15.022297	2.860832
7	0.1396	12.870105	3.897632
8	0.1595	11.264368	5.08805
9	0.1795	10.009285	6.44405
10	0.1994	9.0103644	7.952072

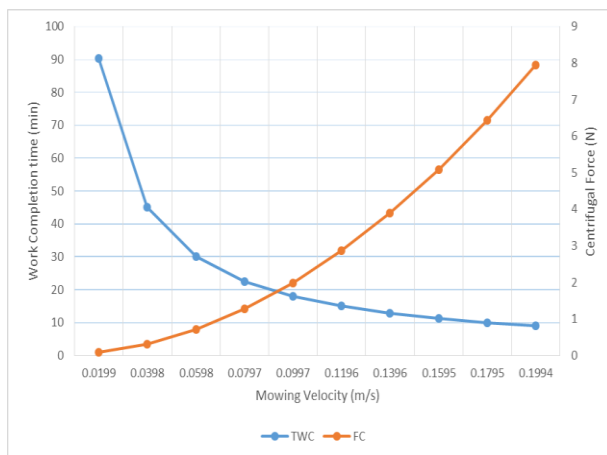


Figure 13. Optimum turning velocity

E. Discussion of Simulation Results

Table III presents performance simulation results of the lawn robot. Table III shows an inverse relationship between mowing velocity and work completion time, while a direct relationship is observed between mowing velocity and centrifugal force. At highest examined mowing velocity of 0.2 m/s, the centrifugal force acting on the robot is approximately 8 N and 9 min work completion time was achieved.

Fig. 13 shows the curve of optimum turning velocity that will minimise the cutting time without deviating from the specified path by the gesture. From Fig. 13, it was observed that curve of work completion time and centrifugal force intersected at 0.096 m/s (optimum turning velocity) which corresponds to centrifugal force of 2 N and work completion time of 20 minutes. This shows that minimal centrifugal force acting on the robot makes it more stable for good cutting and this impacts on the cutting time [21-23]

V. CONCLUSIONS

The work has presented the development of a solar lawn cutting robot adapted for a partially structured environment. The major operational performance objectives of maximum covered area, lawn availability and energy

consumption were achieved via implementation of a solar powered design and hand gesture control module. Incorporation of hand gesture identification and control has really improved the planning of the path and obstacle avoidance mechanism of the robot taking into account its kinematic constraint, thus reducing the work completion time drastically as the mowing velocity was properly managed.

CONFLICT OF INTEREST

The authors declare no conflict of interest.

AUTHOR CONTRIBUTIONS

Adefemi Adeodu conducted the experimentation and wrote the manuscript; Rendani Maladzhi analyzed the data; Mukondeleli G. Kana-kana Katumba executed the simulation. All authors had approved the final version.

FUNDING

The authors wish to thank the Department of Mechanical Engineering, University of South Africa. The work was supported with Departmental research output Fund.

REFERENCES

- [1] A. O. Adeodu, I. A. Daniyan, T. S. Ebimoghan, S. O. Akinola, "Development of an embedded obstacle avoidance and path planning autonomous solar grass cutting robot for semi-structured," *Environment. IEEE Xplore Digital Library*. 2018. Doi:10.1109/ICASTECH.2018.8506681
- [2] S. H. Bhutada and G. U. Shinde, "Design modification and performance comparison of lawn mower machine by mulch and flat type cutting blade," *International Journal of Agricultural Sciences*, vol. 9, no. 40, pp. 4638-4641. 2017.
- [3] S. Chauhan, "Motor torque calculations for electric vehicle," *International Journal of Scientific & Technology Research*, vol. 4, no. 8, pp. 126-127, 2015.
- [4] S. G. Chouhan, S. A. Shaik, K. V Krishnareedy, and S. R. Bandaru. "Design of a power autonomous solar powered lawn mower," *International Journal of Mechanical Engineering and Technology*, vol. 8, no. 5. pp. 1-11. 2017.
- [5] A. Sultema, S. Fatima, H. Mubeen, R. Began, K. Soheltama, and A. Jameel, "A review on smart IOT based gesture controlled grass cutting robot," in *Proc. 4th International Conference on Trends in Electronics and Informatics (ICOET)*, June 15-20, India. Doi. 1109/1COE148184.2020.142981
- [6] G. Du and P. Zhang, "A markerless human-robot interface using particle filter and Kalman filter for dual robots," *IEEE Transactions on Industrial Electronics*, vol. 62, no. 4, April 2015, pp. 2257-2264.
- [7] D. Haessig, J. Hwang, S. Gallagher, M. Uhm, "Case-study of a Xilinx system generator design flow for rapid development of SDR waveforms," in *Proc. the SDR 05 Technical Conference and Product Exposition*, Copyright © 2005 SDR Forum.
- [8] S. Kar, et al. "Image processing based customized image editor and gesture controlled embedded robot coupled with voice control feature," *International Journal of Advance Computer Science and Application*, vol. 6, no 11. 2015.
- [9] Y. Dong, H. Ma, X. Hu, Y. Sun, and Y. Zhu, "Design and production for automatic tracking system of portable solar panel," in *Proc. 2019 International Conference on Robots & Intelligent System (ICRIS)*, 2019, pp. 18-21.
- [10] C. Li, H. Ma, C. Yang, and M. Fu, "Teleoperation of a virtual iCub robot under framework of parallel flow for hand gesture recognition," in *Proc. 2014 IEEE International Conference on Fuzzy Systems*, Beijing, 2014, pp. 1469-1474.

- [11] Z. MA and P. Ben-Tzvi, "RML Glove—An exoskeleton glove mechanism with haptics feedback," *IEEE/ASME Transactions on Mechatronics*, vol. 20, no. 2, pp. 641-652, April 2015.
- [12] M. Moore, "A DSP-based real time image processing system," in *Proc. the 6th International Conference on Signal Processing Applications and Technology*, Boston MA, August 1995.
- [13] W. Zhang, H.Cheng, L. Zhao, L. Hao, M.Tao, C. Xiang, "A gesture based teleoperation system for compliant robot motion," *Applied Science*, vol. 9, no. 24, 5290. 2019. Doi.org/10.3390/app 9243290
- [14] J. L. Raheja, B. Ajay, and A. Chaudhary, "Real time fabric defect detection system on an embedded DSP platform," *Optik: International Journal for Light and Electron Optics*, Elsevier, vol. 124, no. 21, 2013, pp. 5280-5284.
- [15] J. L. Raheja, G. A. Rajsekhar, and A. Chaudhary, "Controlling a remotely located Robot using Hand Gestures in real time: A DSP implementation," in *Proc. 5th IEEE International conference on Wireless Network and Embedded Systems*, India, Oct. 16-17, 2016, pp. 1-5.
- [16] J. L. Raheja, R. Shyam, G. A. Rajsekhar, and P. B. Prasad, "Real-time robotic control using hand gesture," *Robotic System-Application, Control and Programming*, In Tech, 2012.
- [17] J. L. Raheja, S. Subramaniyam, and A. Chaudhary, "Real-time hand gesture recognition in FPGA," *Optik: International Journal for Light and Electron Optics*, vol. 127, no. 20, pp. 9719-9726, 2016.
- [18] M. R. Raihan, R. Hasan, F. Arifin, S. Nashif, and M. R. Haider, "Design and implementation of a hand movement controlled robotic vehicle with wireless live streaming feature," in *Proc. 2019 IEEE International Conference on System Computation Automation and Networking (ICSCAN)*, pp. 1-6, 2019. [USPTO Patent, Application No. 20080256494, 10/16/08
- [19] R. Verma and A. Dev, "Vision based hand gesture recognition using finite state machines and fuzzy logic," in *Proc. International Conference on Ultra-Modern Telecommunications & Workshops*, 12-14 Oct. 2009, pp. 1-6, in St. Petersburg, Russia.
- [20] Y. Wu and T. S. Huang, "Vision based gesture. recognition: A review, lecture notes in computer science," vol. 1739, in *Proc. the International Gesture Workshop on Gesture-Based Communication in Human-Computer Interaction*, 1999.
- [21] Arduino Nano | Arduino Official Store, [Online] Available: <https://store.arduino.cc/usa/arduino-nano>. 2020
- [22] Lawnmowerguide. [Online] Available: <http://www.lawnmowerguide.com/>
- [23] T. Tahir, A. Khalid, J. Arshad, A. Haider, I. Rasheed, A. Rehman, S. Hussan, "Implementation of IOT-Baded Solar Powered Smart Lawn Mower" *Wireless Communication and Mobile Computing*. Volume 2022 | Article ID 1971902 | <https://doi.org/10.1155/2022/1971902>

Copyright © 2023 by the authors. This is an open access article distributed under the Creative Commons Attribution License (CC BY-NC-ND 4.0), which permits use, distribution and reproduction in any medium, provided that the article is properly cited, the use is non-commercial and no modifications or adaptations are made.